

Time Delays in Two-Photon Ionization

Jing Su, Hongcheng Ni, Agnieszka Jaroń-Becker, and Andreas Becker

JILA and Department of Physics, University of Colorado, Boulder, Colorado 80309-0440, USA
(Received 8 April 2014; revised manuscript received 24 July 2014; published 24 December 2014)

We present results of *ab initio* numerical simulations of time delays in two-photon ionization of the helium atom using the attosecond streaking technique. The temporal shifts in the streaking traces consist of two contributions, namely, a time delay acquired during the absorption of the two photons from the extreme-ultraviolet field and a time delay accumulated by the photoelectron after photoabsorption. In the case of a nonresonant transition, the absorption of the two photons is found to occur without time delay. In contrast, for a resonant transition a substantial absorption time delay is found, which scales linearly with the duration of the ionizing pulse. The latter can be related to the phase acquired during the transition of the electron from the initial ground state to the continuum and the influence of the streaking field on the resonant structure of the atom.

DOI: 10.1103/PhysRevLett.113.263002

PACS numbers: 32.80.Fb, 32.80.Rm

Advances in the understanding of the interaction of intense laser pulses with matter have led to the observation of a plethora of new phenomena and the development of new technologies. Among this, the generation of ultrashort extreme-ultraviolet (XUV) laser pulses with ever-shorter duration via high-order harmonic generation is one exciting trend [1]. The availability of (isolated) attosecond (1 as = 10^{-18} s) laser pulses [2–4] has opened the perspective to temporally resolve the dynamics of electrons in atoms, molecules, and solids [5–10]. One of the key methods for such time-resolved measurements is the attosecond streaking technique [11], in which the momentum of a photoelectron, ionized by an isolated attosecond XUV laser pulse, is changed by a superimposed infrared streaking pulse. Observation of the momentum, or energy, of the photoelectron as a function of the phase of the streaking pulse, at which the center of the ionizing XUV pulse is applied, provides the streaking trace.

In streaking experiments on the photoionization of atoms [5] and solids [6], temporal shifts between different streaking traces have been observed. When the traces are compared with the vector potential of the streaking pulse, the shifts can be interpreted as time delays accumulated by the photoelectron after its transition into the continuum. This continuum time delay is determined by the photoelectron dynamics in the combined potential of the Coulomb and streaking fields over a finite range in space until the streaking pulse ceases [12–14]. For atomic photoionization, the continuum time delay can be usually represented (e.g., Refs. [15–20]) by a sum of the (short-range) Wigner-Smith time delay (e.g., Refs. [21–26]) and a time delay (e.g., Refs. [15,16,18,27]) induced by the coupling of the long-range Coulomb tail and the streaking field.

Below, we show that the advanced understanding of the continuum time delay opens the perspective to retrieve time-resolved information during the transition of the electron

into the continuum. To this end, we consider two-photon ionization (TPI) of the helium atom (see Fig. 1) and a model system and perform *ab initio* simulations to obtain streaking time delays Δt_s for different scenarios. We interpret the results as such that for nonresonant TPI the temporal shifts in streaking traces can be understood as solely due to the continuum time delay Δt_c . In contrast, we find a substantial difference between the streaking temporal shift Δt_s and the continuum time delay Δt_c for a resonant transition. We interpret this deviation as an additional time delay Δt_a , acquired during the transition into the continuum.

To simulate the streaking process, we use the Crank-Nicolson method to numerically solve the corresponding

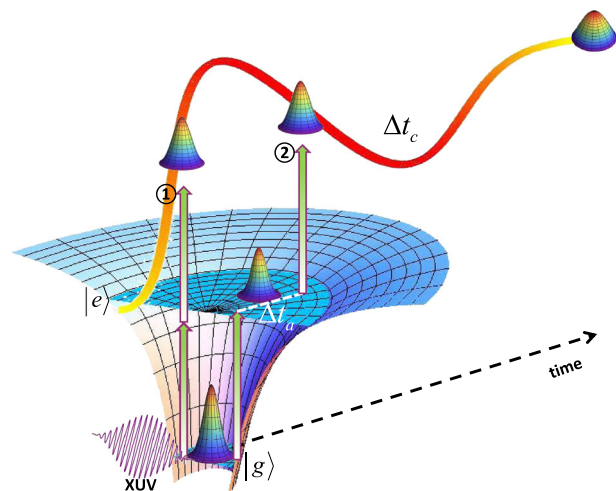


FIG. 1 (color online). Time delays in attosecond streaking of ① nonresonant and ② resonant TPI by an ultrashort XUV laser pulse. The streaking time delay Δt_s , obtained from the streaking trace consists of two contributions, namely, the two-photon absorption time delay Δt_a and the continuum time delay Δt_c that the photoelectron accumulates in the continuum after photoabsorption.

time-dependent Schrödinger equation (TDSE) on a grid in space and time (Hartree atomic units, $e = m = \hbar = 1$, are used unless stated otherwise),

$$i\frac{\partial\Psi(\mathbf{r},t)}{\partial t} = \left[\frac{\mathbf{p}^2}{2} + V(\mathbf{r}) + [\mathbf{E}_X(t) + \mathbf{E}_s(t)] \cdot \mathbf{r} \right] \Psi(\mathbf{r},t), \quad (1)$$

where \mathbf{p} is the momentum operator and $\mathbf{E}(t) = E_0 \cos^2(\pi t/T) \cos(\omega t + \phi) \hat{\mathbf{z}}$ with peak amplitude E_0 , pulse duration T , central frequency ω , and carrier-envelope phase ϕ is used for both the ionizing (\mathbf{E}_X) and the streaking (\mathbf{E}_s) fields. In all simulations, we propagate the wave function on the grid for a sufficiently long time until both laser pulses have ceased and the ionizing wave packet can be clearly separated from the remaining bound part of the wave function. The extensions of the grid $[0, 960]$ in the ρ direction and $[-1100, 1100]$ in the z direction for the three-dimensional (3D) He atom, $[-7000, 7000]$ for the one-dimensional (1D) Coulomb potential] are chosen such that the outgoing wave packet remains on the grid and does not reach the boundaries. The momentum distributions are obtained by projecting the ionizing wave function onto the continuum eigenstates of the potential or by performing a Fourier transform. Results of both methods are found to agree well with each other.

We simulate the TPI process dressed by a streaking field for a helium atom (He) in the 3D cylindrical coordinates as well as for a 1D Coulomb model potential. For colinear polarization of the two fields, the calculations for the He atom reduce to 2D (ρ and z coordinates) because of the azimuthal symmetry of the problem. Using spatial steps of $\Delta\rho = \Delta z = 0.2$ and a time step of $\Delta t = 0.02$, we obtain eigenenergies of the three lowest states as $E_{1s} = -0.90$, $E_{2s} = -0.16$, and $E_{2p} = -0.13$, using the single-active-electron model potential introduced in Ref. [28] and imaginary time propagation. To ionize the electron initially bound in the $1s$ state via the absorption of two photons, we choose the central frequency of the XUV field to be $\omega_X = 15.63$ or 21.07 eV. The latter resonant frequency corresponds to the energy difference between the $1s$ and $2p$ states in the He atom potential. Since the streaking field may have a non-negligible effect on the electronic structure of the He atom, we have furthermore considered a simple 1D Coulomb potential of the form $V(x) = -Z/\sqrt{x^2 + a}$ with $Z = 3.0$ and $a = 0.15$ and the energies of the three lowest states $E_1 = -5.32$, $E_2 = -2.31$, and $E_3 = -1.30$, for $\Delta x = 0.05$ and $\Delta t = 0.01$. Accordingly, we have chosen $\omega_X = 95.62$ and 81.81 eV, corresponding to non-resonant and resonant TPI processes. The 1D model system provides us the opportunity to selectively study the ionization via the deeply bound first excited state only, which is not influenced by the streaking field. In comparison with the case of the 3D He atom, we can therefore identify the potential effects of the streaking field on the resonant two-photon absorption process. Other parameters for the XUV

pulse are chosen as $I_X = 1.0 \times 10^{14}$ (nonresonant transitions) or 1.0×10^{13} W/cm² (resonant transitions), and $\phi_X = -\pi/2$ in all calculations. In order to keep the duration of the XUV pulse shorter than the oscillation period of the streaking pulse, we have used a three-cycle streaking field of at least 2400 nm in wavelength with $I_s = 1.0 \times 10^{11}$ W/cm² and $\phi_s = -\pi/2$.

In Fig. 2 we present results of time delays retrieved from the numerical streaking simulations. To this end, we have applied the ionizing XUV pulse at different phases (in time steps of 12.0 a.u.) of the streaking pulse, solved the TDSE, and recorded the momentum distribution of the photoelectron. The streaking time delay has then been obtained as the temporal offset between the streaking trace, i.e., the momentum distributions as a function of the phase of the streaking pulse, and the vector potential of the streaking pulse [13]. In each panel of Fig. 2 we show the streaking time delays as a function of the XUV pulse duration for resonant (green lines with squares) and nonresonant (blue lines with circles) ionization. The trends of the time delays are obviously different. In the case of resonant TPI, the streaking time delay increases with T_X , at long XUV pulse durations linearly with the increase of T_X . In contrast, for a nonresonant TPI, the streaking time delay remains almost unchanged, in particular at longer pulse durations. To contrast our present results with those for single-photon ionization (SPI), we have performed simulations with XUV pulses having central frequencies equal to twice that of the corresponding nonresonant TPI processes. The peak intensities of the XUV pulse are $I_X = 1.0 \times 10^{14}$ W/cm² for the 1D Coulomb potential and $I_X = 1.0 \times 10^{12}$ W/cm² for the He atom. Similar to the case in the nonresonant TPI process, the retrieved SPI streaking time delays are nearly independent of the XUV pulse duration (Fig. 2). For the 3D He atom, these two time delays are not exactly equivalent, since in SPI and TPI the photoelectron has different angular momenta in the continuum (p wave for SPI, and a mixture of s and d waves for TPI), which results in different streaking time delays (e.g., Refs. [15,18]).

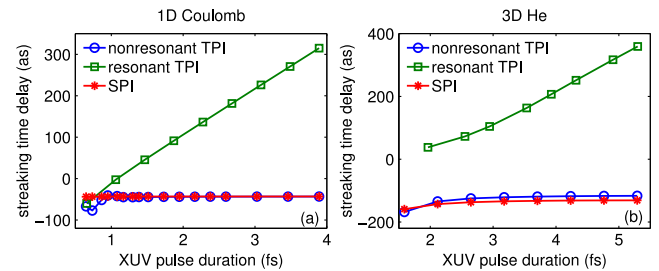


FIG. 2 (color online). Streaking time delay as a function of XUV pulse duration for (a) 1D Coulomb and (b) 3D He potentials. Three ionization processes are considered: nonresonant TPI (blue lines with circles), resonant TPI (green lines with squares), and single-photon ionization (red lines with asterisks). Laser parameters are given in the text.

Thus, the results show that in a resonant transition a significant additional time delay that depends on the XUV pulse parameters is acquired by the electron. We assume that this additional time delay is accumulated during the transition to the continuum via the resonant excited state and postulate that the retrieved streaking time delay Δt_s consists of two contributions as

$$\Delta t_s = \Delta t_c + \Delta t_a, \quad (2)$$

where Δt_c is the continuum time delay, accumulated by the photoelectron *after* the transition into the continuum during its propagation in the combined Coulomb-streaking field until the streaking pulse ceases [12,13]. Δt_a is the time delay accumulated *during* the transition of the electron from the initial state into the continuum, which we denote as absorption time delay, since the transition is related to the absorption of the photons.

It has been shown that Δt_c can be well determined using classical-trajectory calculations [12,15]. For the 1D Coulomb potential we solve the 1D Newton's equation for the combined Coulomb-streaking field from an initial position of the electron at $x = 0$ [12]. The obtained continuum time delays are shown as green lines with squares in Figs. 3(a) and 3(c). For the He atom, we use the classical-trajectory Monte Carlo method introduced in Ref. [15], in which the initial position and momentum of the electron are sampled using the probability distribution of the initial eigenstate and the momentum distribution according to the angular shape of the wave packet (either *s* or *d* wave), respectively. The continuum time delays

obtained for the *s* and *d* wave distributions are added up according to their respective probabilities [green lines with squares in Figs. 3(b) and 3(d)]. Since the central energy of the photoelectron that mainly determines the continuum time delay barely changes with the XUV pulse duration, the results for Δt_c are almost independent of T_X .

Now we are able to obtain the absorption time delays Δt_a , shown as red lines with asterisks in Fig. 3, via Eq. (2). In agreement with our qualitative expectations above, for long XUV pulses the absorption time delays are found to be (close to) zero in the case of nonresonant TPI. This implies that the transition of the electron from the initial state into the continuum occurs instantaneously without any time delay. In contrast, we find a significant absorption time delay for the resonant TPI processes, which changes linearly with the XUV pulse duration, once the pulse is long enough. Because of the large bandwidth of the pulse and related excitations to multiple states, a deviation from the linear and constant trends is observed for the short pulse durations [see Figs. 3(b) and 3(d)].

In order to further support our interpretation, we show that the retrieved absorption time delay is, indeed, related to the energy derivative of the phase that the electron acquires in the transition from the initial state to the continuum. On the basis of second-order time-dependent perturbation theory, the complex amplitude c_f of the ionizing wave packet in the continuum state $|f\rangle$ ionized from the initial state $|i\rangle$ after the XUV pulse ceases can be written as [29]

$$c_f = \sum_m \mu_{fm} \mu_{mi} \int_{-(T/2)}^{T/2} e^{i\Delta_{fm}t} E(t) \left(\int_{-(T/2)}^t e^{i\Delta_{mi}t'} E(t') dt' \right) dt, \quad (3)$$

where T is the duration of the XUV pulse $E(t)$ and $\mu_{jk} = E_j - E_k$ are the dipole transition matrix element and the energy difference between states $|j\rangle$ and $|k\rangle$, respectively. For nonresonant TPI, assuming that all intermediate states are outside the bandwidth of the XUV pulse, we can further simplify Eq. (3) as [30,31]

$$c_f \propto a_f \approx \int_{-(T/2)}^{T/2} e^{i\Delta_{fi}t} E^2(t) dt, \quad (4)$$

where we have dropped the dipole matrix element since the corresponding phase is related to the scattering (or propagation) of the electron in the continuum, which is accounted for in the continuum time delay. For resonant TPI, we can rewrite Eq. (3) as

$$c_f \propto a_f \approx \int_{-(T/2)}^{T/2} e^{i\Delta_{fi}t} E(t) \left(\int_{-(T/2)}^t e^{i\Delta_{ri}t'} E(t') dt' \right) dt, \quad (5)$$

assuming that only one state $|r\rangle$ is within the XUV pulse bandwidth. The absorption time delay can then be related to the phase of the complex amplitude as (e.g., Refs. [23,24])

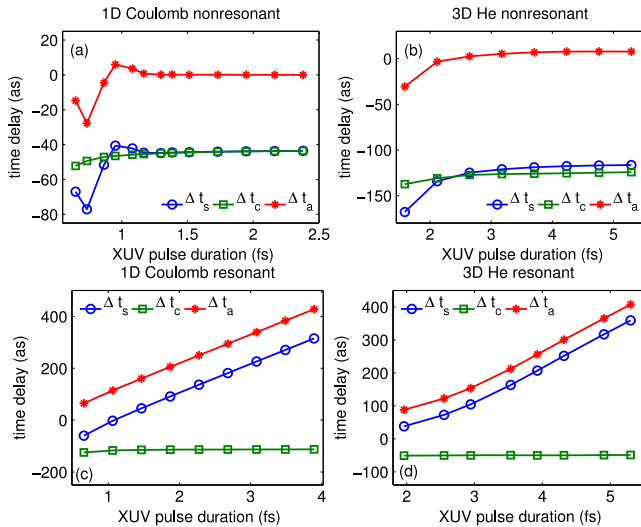


FIG. 3 (color online). Absorption time delay (red lines with asterisks) as a function of XUV pulse duration for nonresonant TPI in 1D Coulomb (a) and 3D He (b) potentials and resonant TPI in 1D Coulomb (c) and 3D He (d) potentials. Also shown are the streaking (blue lines with circles) and the continuum time delays (green lines with squares).

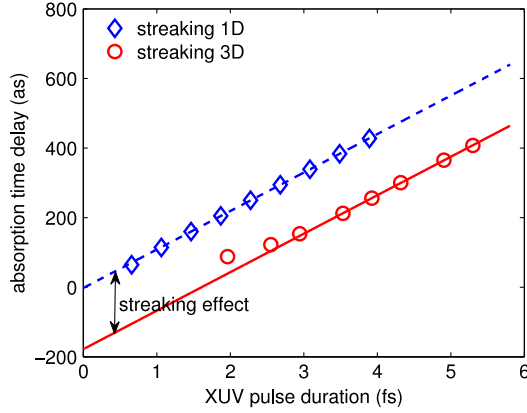


FIG. 4 (color online). Comparison of absorption time delays extracted from streaking experiments for resonant TPI in the 1D model potential (blue diamonds) and the 3D He potential (red circles). Two fits $\Delta t_a = 110.6T - 2.175$ (1D case, dashed line) and $\Delta t_a = 110.6T - 178.0$ (3D case, solid line) account for the predicted linear trend of the delay as a function of the XUV pulse duration.

$$\Delta t_a = \frac{d}{dE} [\arg(a_f)]. \quad (6)$$

For a \cos^2 XUV profile considered in our simulations, Eq. (6) can be evaluated numerically and Δt_a is found (not shown) to be equal to zero in the nonresonant case, while it changes linearly with the pulse duration in the resonant case, in agreement with our findings from the streaking calculations.

Our analytical evaluation of the absorption time delay does not account for any influence of the streaking pulse on the resonant structure of the atom. Previous studies of two-color resonant two-photon ionization have, however, shown that the effect is not negligible [32]. From our numerical results, we can quantify it by comparing the results for the absorption time delays, extracted from the numerical streaking calculations, for the 1D model potential and the 3D He atom potential in Fig. 4. Two linear fits to the results in the regime of large pulse durations are shown as solid (for the He atom case) and dashed (for the 1D model potential) lines, respectively. We may stress that the obtained absorption time delays for resonant TPI in the case of the 1D model potential are found to be independent of the parameters of the streaking pulse, as shown in Table I. In contrast, the streaking time delays (and the continuum time delays) vary with the wavelength and intensity of the streaking pulse. This shows that, as expected, the deeply bound first excited state of the 1D model potential is not influenced by the streaking field. Consequently, in this case the linear fit (dashed line) for the absorption time delay extends to zero when the XUV pulse duration approaches zero, as predicted by our theoretical analysis above. However, the results for Δt_a in the case of the 3D He atom potential show a constant offset that can be

TABLE I. Time delays for different parameters of the streaking field. We consider resonant TPI in the 1D Coulomb potential streaked by a three-cycle laser pulse. XUV laser parameters are $\omega_X = 81.81$ eV, $N_X = 45$, $I_X = 1.0 \times 10^{13}$ W/cm², and $\phi_X = -\pi/2$.

λ_s (nm)	I_s (W/cm ²)	Δt_s (a.u.)	Δt_a (a.u.)
2400	1.0×10^{11}	5.65	10.34
3200	1.0×10^{11}	5.15	10.34
4800	1.0×10^{11}	4.41	10.33
4800	1.0×10^{10}	4.45	10.36

read from the intersection of the linear fit (solid line) at zero XUV pulse duration (in the present case, 178 as). We interpret this as a quantification of the influence of the streaking field on the resonant $2p$ state.

In summary, we have studied time delays in the photo-absorption of nonresonant and resonant TPI using the attosecond streaking technique. By accounting for the continuum time delay, we find that the absorption time delay is zero for nonresonant TPI, while for resonant TPI it is nonzero and changes linearly with the duration of the ionizing XUV pulse. The absorption time delays can be understood by analyzing the phase in the two-photon absorption process using second-order perturbation theory. For the experimental realization, we propose to compare streaking traces for resonant (nonresonant) TPI from an inner-valence shell orbital of an atom (e.g., the $2s$ orbital in Ne) with the streaking trace for SPI from the outermost orbital of the same atom (e.g., the $2p$ orbital in Ne) induced by an isolated attosecond pulse. According to our results, for a given pulse duration, the comparison with the SPI trace should reveal a substantial difference in the streaking delays for resonant vs nonresonant TPI. The difference in the absorption delays can then be extracted from the streaking time delays using the well-known theoretical approaches [12,20] to account for the continuum time delays. If, furthermore, a variation of the XUV pulse duration is possible, the linear dependence of the streaking delay for resonant TPI (as compared to the nearly constant reference streaking delay for SPI) should become observable. The required pulse lengths should be available using the technique of isolation of XUV pulses via phase matching in high-order harmonic generation at midinfrared driver wavelengths [4]. Laser pulses at infrared wavelengths, which are used for strong-field ionization [33] and higher-order harmonic generation [34] already, are in the present approach needed for the streaking field as well. The energy range of the XUV pulses corresponds to below-threshold harmonics that recently attracted attention in the experiment [35,36].

We thank Phil Bucksbaum for stimulating discussions. J. S. and A. B. acknowledge support by a grant from the U.S. Department of Energy, Division of Chemical Sciences, Atomic, Molecular and Optical Sciences

Program (Award No. DE-FG02-09ER16103). H.N. was supported via grants from the U.S. National Science Foundation (Grants No. PHY-0854918 and No. PHY-1125844). A.J.-B. was supported by grants from the U.S. National Science Foundation (Grants No. PHY-1125844 and No. PHY-1068706). This work utilized the Janus supercomputer, which is supported by the National Science Foundation (Grant No. CNS-0821794) and the University of Colorado, Boulder. The Janus supercomputer is a joint effort of the University of Colorado, Boulder, the University of Colorado, Denver, and the National Center for Atmospheric Research. Janus is operated by the University of Colorado, Boulder.

-
- [1] T. Popmintchev, M. C. Chen, P. Arpin, M. M. Murnane, and H. C. Kapteyn, *Nat. Photonics* **4**, 822 (2010).
- [2] I. P. Christov, M. M. Murnane, and H. C. Kapteyn, *Phys. Rev. Lett.* **78**, 1251 (1997).
- [3] E. Goulielmakis, M. Schultze, M. Hofstetter, V. S. Yakovlev, J. Gagnon, M. Uiberacker, A. L. Aquila, E. M. Gullikson, D. T. Attwood, R. Kienberger, F. Krausz, and U. Kleineberg, *Science* **320**, 1614 (2008).
- [4] M. C. Chen, C. Hernández-García, C. Manusco, F. Dollar, B. Galloway, D. Popmintchev, P.-C. Huang, B. Walker, L. Plaja, A. Jaroń-Becker, A. Becker, T. Popmintchev, M. M. Murnane, and H. C. Kapteyn, *Proc. Natl. Acad. Sci. U.S.A.* **111**, E2361 (2014).
- [5] M. Schultze, M. Fieß, N. Karpowicz, J. Gagnon, M. Korbman, M. Hofstetter, S. Neppl, A. L. Cavalieri, Y. Komninos, T. Mercouris, C. A. Nicolaides, R. Pazourek, S. Nagele, J. Feist, J. Burgdörfer, A. M. Azzeer, R. Ernstorfer, R. Kienberger, U. Kleineberg, E. Goulielmakis, F. Krausz, and V. S. Yakovlev, *Science* **328**, 1658 (2010).
- [6] A. L. Cavalieri, N. Müller, Th. Uphues, V. S. Yakovlev, A. Baltuska, B. Horvath, B. Schmidt, L. Blümel, R. Holzwarth, S. Hendel, M. Drescher, U. Kleineberg, P. M. Echenique, R. Kienberger, F. Krausz, and U. Heinzmann, *Nature (London)* **449**, 1029 (2007).
- [7] E. Gagnon, P. Ranitovic, X.-M. Tong, C. L. Cocke, M. M. Murnane, H. C. Kapteyn, and A. S. Sandhu, *Science* **317**, 1374 (2007).
- [8] K. Klünder, J. M. Dahlström, M. Gisselbrecht, T. Fordell, M. Swoboda, D. Guenot, P. Johnsson, J. Caillat, J. Mauritsson, A. Maquet, R. Taieb, and A. L'Huillier, *Phys. Rev. Lett.* **106**, 143002 (2011).
- [9] S. Mathias, C. La-O-Vorakiat, P. Grychtol, P. Granitzka, E. Turgut, J. M. Shaw, R. Adam, H. T. Nembach, M. Siemens, S. Eich, C. M. Schneider, T. J. Silva, M. Aeschlimann, M. M. Murnane, and H. C. Kapteyn, *Proc. Natl. Acad. Sci. U.S.A.* **109**, 4792 (2012).
- [10] D. Rudolf, C. La-O-Vorakiat, M. Battiato, R. Adam, J. J. Shaw, E. Turgut, P. Maldonado, S. Mathias, P. Grychtol, H. T. Nembach, T. J. Silva, M. Aeschlimann, H. C. Kapteyn, M. M. Murnane, C. M. Schneider, and P. M. Oppeneer, *Nat. Commun.* **3**, 1037 (2012).
- [11] J. Itatani, F. Quéré, G. L. Yudin, M. Y. Ivanov, F. Krausz, and P. B. Corkum, *Phys. Rev. Lett.* **88**, 173903 (2002).
- [12] J. Su, H. Ni, A. Becker, and A. Jaroń-Becker, *Phys. Rev. A* **88**, 023413 (2013).
- [13] J. Su, H. Ni, A. Becker, and A. Jaroń-Becker, *Phys. Rev. A* **89**, 013404 (2014).
- [14] J. Su, H. Ni, A. Becker, and A. Jaroń-Becker, *Chin. J. Phys. (Taipei)* **52**, 404 (2014).
- [15] S. Nagele, R. Pazourek, J. Feist, K. Doblhoff-Dier, C. Lemell, K. Tökési, and J. Burgdörfer, *J. Phys. B* **44**, 081001 (2011).
- [16] M. Ivanov and O. Smirnova, *Phys. Rev. Lett.* **107**, 213605 (2011).
- [17] S. Nagele, R. Pazourek, J. Feist, and J. Burgdörfer, *Phys. Rev. A* **85**, 033401 (2012).
- [18] J. M. Dahlström, A. L'Huillier, and A. Maquet, *J. Phys. B* **45**, 183001 (2012).
- [19] J. M. Dahlström, D. Guénot, K. Klünder, M. Gisselbrecht, J. Mauritsson, A. L'Huillier, A. Maquet, and R. Taëb, *Chem. Phys.* **414**, 53 (2013).
- [20] R. Pazourek, S. Nagele, and J. Burgdörfer, *Faraday Discuss.* **163**, 353 (2013).
- [21] E. P. Wigner, *Phys. Rev.* **98**, 145 (1955).
- [22] F. T. Smith, *Phys. Rev.* **118**, 349 (1960).
- [23] A. S. Kheifets and I. A. Ivanov, *Phys. Rev. Lett.* **105**, 233002 (2010).
- [24] I. A. Ivanov, *Phys. Rev. A* **83**, 023421 (2011).
- [25] C.-H. Zhang and U. Thumm, *Phys. Rev. A* **84**, 033401 (2011).
- [26] I. A. Ivanov, *Phys. Rev. A* **86**, 023419 (2012).
- [27] C.-H. Zhang and U. Thumm, *Phys. Rev. A* **82**, 043405 (2010).
- [28] X. M. Tong and C. D. Lin, *J. Phys. B* **38**, 2593 (2005).
- [29] K. L. Ishikawa and K. Ueda, *Phys. Rev. Lett.* **108**, 033003 (2012).
- [30] D. Meshulach and Y. Silberberg, *Nature (London)* **396**, 239 (1998).
- [31] D. Meshulach and Y. Silberberg, *Phys. Rev. A* **60**, 1287 (1999).
- [32] M. Swoboda, T. Fordell, K. Klünder, J. M. Dahlström, M. Miranda, C. Buth, K. J. Schafer, J. Mauritsson, A. L'Huillier, and M. Gisselbrecht, *Phys. Rev. Lett.* **104**, 103003 (2010).
- [33] C. I. Blaga, F. Catoire, P. Colomison, G. G. Paulus, H. G. Muller, P. Agostini, and L. F. DiMauro, *Nat. Phys.* **5**, 335 (2009).
- [34] T. Popmintchev, M.-C. Chen, D. Popmintchev, P. Arpin, S. Brown, S. Alisauskas, G. Andriukaitas, T. Balciunas, O. D. Mücke, A. Pugzlys, A. Baltuska, B. Shim, S. E. Schrauth, A. Gaeta, C. Hernandez-Garcia, L. Plaja, A. Becker, A. Jaron-Becker, M. M. Murnane, and H. Kapteyn, *Science* **336**, 1287 (2012).
- [35] M. Chini, X. Wang, Y. Cheng, H. Wang, Y. Wu, E. Cunningham, P.-C. Li, J. Heslar, D. Telnov, S.-I. Chu, and Z. Chang, *Nat. Photonics* **8**, 437 (2014).
- [36] C. Benko, T. K. Allison, A. Cingöz, L. Hua, F. Labaye, D. C. Yost, and J. Ye, *Nat. Photonics* **8**, 530 (2014).